Food Chemistry: X 21 (2024) 101076

Contents lists available at ScienceDirect

Food Chemistry: X

journal homepage: www.sciencedirect.com/journal/food-chemistry-x

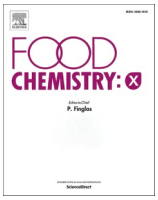

Bioactivity and influence on colonic microbiota of polyphenols from noni (*Morinda citrifolia* L.) fruit under simulated gastrointestinal digestion

Juanyun Chen [a,b,c], Xiaoai Chen [a,b,*], Yanjun Zhang [a,b], Zhen Feng [a,b], Kexue Zhu [a,b], Fei Xu [a,b], Chunhe Gu [a,b,*]

[a] *Spice and Beverage Research Institute, Chinese Academy of Tropical Agricultural Sciences, Wanning 571533, Hainan, China*
[b] *Key Laboratory of Processing Suitability and Quality Control of the Special Tropical Crops, Wanning 571533, Hainan, China*
[c] *College of Food Science & Technology, Huazhong Agricultural University, Wuhan 430070, Hubei, China*

ARTICLE INFO

Keywords:
Noni fruit
Ripeness level
Polyphenol
Antioxidant activity
Gut microbiome

ABSTRACT

Noni (*Morinda citrifolia* L.) is a tropical fruit rich in bioactive compounds. Little is known about its polyphenol composition at different ripeness levels and digestive characteristics. Here, we studied changes in polyphenols and antioxidant activity as noni ripened. Rutin and kaempferol-3-*O*-rutinoside were found in high amounts in noni, with antioxidant capacity increasing as it ripened. Under simulated digestion, polyphenols were gradually released from the oral to gastrointestinal phases, partially decomposing in the small intestine due to their instability. Conversely, fiber-bound phenols were released during colonic fermentation, leading to high bioaccessible antioxidant activity. Additionally, noni consumption affected the intestinal microbiome by reducing the Firmicutes/Bacteroidetes ratio and increasing bacteria with prebiotic properties like *Prevotella* and *Ruminococcus*. These findings demonstrate that polyphenols significantly contribute to the health benefits of noni fruit by providing absorbable antioxidants and improving the structure of the intestinal microbiome.

Introduction

Noni (*Morinda citrifolia* L.) is a fruit belonging to the Rubiaceae family and is primarily found in South and Southeast Asia. It has been traditionally consumed as a food and medicinal plant and is now marketed worldwide as a dietary supplement (Pratap et al., 2017). Noni fruit is a rich source of bioactive compounds and has been extensively studied in recent years, with over 200 phytochemicals identified (Motshaker and Ghazali, 2015). The majority of these compounds have been found to have significant health benefits, including anti-tumor, anti-diabetic, anti-obesity, antibacterial, antiseptic, antiviral, anti-inflammatory, and anti-cancer properties (Tailulu et al., 2022).

Polyphenols are the primary contributors to antioxidant bioactivity, and are widely found in fruits and vegetables. Over 8,000 phenolic compounds have been identified and studied extensively for their medicinal properties. Epidemiological studies have shown that long-term exposure to polyphenol-rich dietary supplements can reduce cellular oxidative stress, and may have protective effects against diseases such as cancer, cardiovascular diseases, diabetes, and neurodegenerative diseases (Kesavan et al., 2018). However, phenolics from different plant sources and those at different ripeness levels can have significantly different digestive patterns in the human gastrointestinal tract (Kesavan et al., 2018). Furthermore, after consumption, only a small percentage (10 %–30 %) of polyphenols from fruits and vegetables are released and absorbed in stomach and small intestine, with the majority of polyphenols being bound to dietary fibers of the plant cell wall. These fiber-bound polyphenols are able to bypass gastric and small intestinal digestion and reach the colon, where they are metabolized by the colonic microbiome (Gu et al., 2020). Therefore, understanding the digestive characteristics of polyphenols release of crucial for the absorption of these compounds. Noni fruit has been found to be rich in bioactive ingredients, with polyphenols being recognized as one of the key contributors to its overall bioactivity (Wang et al., 2022), yet the phenolic profile of noni fruit at different ripeness stages and its digestive and metabolic behavior remains largely unclear. Based on the bioactive substances present in noni fruit and its traditional use as a medical food for treating hypertension, diabetes, hyperlipidemia etc. (Édipo et al., 2019), it is hypothesized that noni fruit could potentially benefit colonic health by virtue of its bioaccessible bioactivity in the gastrodigestive system, as well as its ability to modulate gut microbiota. This study aims

* Corresponding authors at: Spice and Beverage Research Institute, Chinese Academy of Tropical Agricultural Sciences, Wanning 571533, Hainan, China.
E-mail address: guchunhe688@163.com (C. Gu).

https://doi.org/10.1016/j.fochx.2023.101076
Received 25 June 2023; Received in revised form 29 November 2023; Accepted 13 December 2023
Available online 16 December 2023

to better understand the bioactivity and digestion of noni fruit by detecting phenolic compounds and subjecting the fruit to simulated in-vitro digestion to observe changes in bioaccessible phenolic compounds and their effects on gut microbiota.

Materials and methods

Materials and reagents

The noni fruit was harvested from Wanning City, Hainan Province, China (18°47′42.51 "N, 110°23′27.86 "E), and was empirically classified by local growers into four levels of ripeness, including unripe, underripe, ripe, and overripe based on the color and texture (Fig. 1) (Chen et al., 2024). More than 20 kg fruit for each level were sampled for the study. After being washed and cut into small pieces, the fruit was juiced using a juice extractor (Kormes, SY-06). The resulting juice was then freeze-dried for 48 h (TFDX 0.25). The freeze-dried powder was sifted through an 80 mesh. Alpha-amylase from porcine pancreas, pepsin and pancreatic enzymes were purchased from Shanghai Yuanye Biotechnology (Shanghai, China), and 1,1-diphenyl-2-picrylhydrazyl (DPPH), 2,4,6-tri(2-pyridyl)-s-triazine (TPTZ) were purchased from Hefei BASF Biotechnology (Hefei, China). 2,2′-azobis[2-methylpropionamidine] dihydrochloride (AAPH) was from Hefei Chansheng Biotechnology, China. All other reagents were of analytical purity and purchased from Xilong Scientific Co., China. Anareopack, oxygen indicator, 2.5 L sealed incubator all were purchased from MitsubishiGroup (Tokyo Port Area, Japan).

Hardness of noni pulp and seeds

The hardness of noni pulp and seeds from fruit at different stages of ripeness was measured according to Shiu et al. (2015). The seeds were separated from the pulp, and the pulp were cut into cubes with 3 cm diameter and 1 cm thickness along the diameter direction. The hardness test was carried out using a TA-XT plus type physical tester (SMS, UK).

Color difference among fruit at different stages of ripeness

Color difference determination was carried out following the protocol outlined by Yuan et al. (2022). The color of noni fruit at different ripeness levels was measured using a colorimeter (Sanenshi Technology Co., Shenzhen, China). The center of each sample was selected, and it was then cut to a size of 0.5 cm × 0.5 cm. The color measurement included three primary factors: L* for the lightness on a scale from black (0) to white (1 0 0), a* from green (−) to red (+), and b* from blue (−) to yellow (+).

Extraction of polyphenols

Polyphenols of the noni fruit were extracted according to the method described by Fahim, Attia & Kamel et al. (2019). The fruit was freeze dried for 24 h and ground into a fine powder. Next, 5 g of noni powder was weighed and extracted with 60 % ethanol (18 mL) at 20 °C for 1 h. The resulting solution was then centrifuged at 4 °C and 10,000 r/min for 20 min, and the supernatant was collected for further measurement of antioxidant activity.

Determination of total polyphenol content

Total phenolic content (TPC) was measured referring to the method of Gu et al. (2020). Here, 10 μL of noni polyphenol extract was taken, 50 μL of Folin-Ciocalteu's reagent was added and placed in dark condition for 5 min, then 100 μL of mass fraction 5 % Na_2CO_3 and 200 μL of ultra-pure water were added. The absorbance at 760 nm (Bio Tek, USA) was measured after incubation for 30 min, and the results were expressed as mg gallic acid equivalent (GAE) per gram of noni powder. All experiments were repeated three times.

Determination of total flavonoids content

Total flavonoid content (TFC) was determined according to the method of Chait, Gunenc, Bendali & Hosseinian (2020). Ten microliter of noni polyphenol extract was taken then added by 50 μL of $NaNO_2$ solution. The mixture then reacted for 5 min immediately avoiding the light. Add $Al(NO_3)_3$ 50 μL to the mixture, react for 5 min avoiding the light, then 500 μL of NaOH was added. The solution was measured at the absorbance of 510 nm (Bio Tek, USA). The results were expressed as mg rutin equivalent (RE) per gram of noni powder, and all tests were repeated three times and the average value was reported.

Determination of scavenging ability of DPPH free radicals

The DPPH free radical antioxidant activity of noni fruit was measured referring to the method of Laya and Koubala (2020). Here, 10 μL of noni extract was taken and fixed to 100 μL with anhydrous ethanol followed by adding 400 μL of 0.25 mmol/L DPPH working solution. The reaction then lasted for 30 min, and the solution was measured at 517 nm using a spectro-photometer (Bio Tek, USA).Each sample was

Fig. 1. Noni fruit at different ripeness levels (unripe, underripe, ripe and overripe) used in the study.

measured three times in parallel to determine the antioxidant capacity to scavenge DPPH radicals of noni fruit powder.

Determination of the scavenging ability of ABTS free radicals

The determination of scavenging ability of ABTS free radicals of noni fruit referred to the method of Gu et al. (2020). The absorbance value of noni extract was measured at the wavelength of 734 nm (Bio Tek, USA). Each sample was measured three times in parallel to determine the scavenging ability of ABTS free radicals of noni fruit powder. The results were expressed as mg ascorbic acid equivalent (AAE) per gram of noni fruit powder.

FRAP assay

The FRAP assay was carried out according to the method of Geng et al.(2023). Here, 50 μL of noni extract sample was added by 900 μL of freshly prepared Ferric ion reducing antioxidant power reagent (FRAP) working solution. The mixture then reacted at 37 °C for 10 min in darkness, and the absorbance was then measured at 595 nm (Bio Tek, USA) with an enzyme standard. Each sample was measured three times and the average value was reported. The results were expressed as g Fe^{2+} per gram of noni fruit powder.

In vitro gastro-intestinal digestion of noni fruit samples

To better simulate the conditions of noni digestion and take dietary fiber-bound polyphenols into consideration, noni powder was used to investigate the metabolism of phenols during digestion. The samples were subjected to a three-stage in vitro digestive process, including oral, gastric and intestinal digestions described by Dong et al. (2021). Simulated intestinal, simulated gastric and simulated saliva fluids (SIF, SGF, SSF) which contains the recommended concentrations of electrolytes were prepared according to the descriptions of Minekus et al. (2014). In the oral section, 0.4 g noni powder was mixed with water, 3.5 mL simulated salivary fluid (SSF), 0.25 mL $CaCl_2$ and 0.5 mL α-amylase (1500 U/mL). The mixture was acidified to a pH of 7.0 with 1 M HCl and incubated at 37 °C for 5 min. In the gastric digestion stage, the oral digest was mixed with 6 mL simulated gastric fluid (SGF), 1 mL porcine pepsin (1500 U/mL). The pH of the mixture was lowered to 1.8 and incubated at 37 °C for 2 h. For the small intestine digestion stage, the gastric digest was mixed with water, 7 mL simulated intestinal fluid (SIF), $CaCl_2$, bile (50 mg) and trypsin (3 mL, 40 U/mL). The pH of the mixture was adjusted to 7.0 by adding 1 M NaOH, followed by stirring for 2 h. Blank experiments without the addition of noni powder were also performed under the same conditions of digestion to correct for interference from the digest, enzyme and liquid. All procedures were carried out under anaerobic conditions with sample containers purged with nitrogen in a shaking incubator at 100 rpm in darkness. The samples was then centrifuged at 10,000 rpm for 10 min at 4 °C, and the resulting supernatant and sediment were frozen at −20 °C and for further analysis. The supernatant was considered as the bioaccessible fraction in the small intestine, whereas the sediment contained the fiber-bound phenols that could potentially reach the colon.

Colonic fermentation

Pig feces were used as sources of gut microbiome as a substitute of human feces, as pigs and humans are primarily colonic fermenters sharing a comparable gut microbiome (Gu et al., 2020). Fresh pig feces was collected from local farmers' homes in Wanning, Hainan. The feces was collected into anaerobic bags immediately after the pigs defecated. Then 20 % fecal slurry was made with sterilized phosphate buffer solution (pH 7.0) after being filtered through sterile gauze.

The basal media was prepared following the method described by Loo et al. (2022) with slight modifications. The content included 2.5 g soluble starch, 2.5 g peptone, 2.5 g tryptone, 2.5 g yeast extract, 2.5 g NaCl, 2.5 g KCl, 1 g pectin, 2 g mucin, 1.5 g casein, 0.75 g $NaHCO_3$, 0.4 g L-Cysteine HCl, 0.6 g MgSO4··$7H_2O$, 0.5 g guar, 0.25 g KH_2PO_4, 0.25 g K_2HPO_4, 0.2 g bile salts, 0.05 g $CaCl_2$ and 1 mL Tween-80. These components were dissolved and added up to 1 L with MilliQ water. The pH of the basal media was then adjusted to 7.0 at 25 °C using 1 mol/L HCl or 1 mol/L NaOH, and the media was sterilized by autoclaving at 121 °C for 15 min. Next, 0.5 g of the lyophilized powder of the sediments from the small intestinal digestion was taken and mixed with 20 % fecal slurry and basal medium. The mixture was maintained under anaerobic conditions with sample containers purged with nitrogen. It was then placed in a shaking incubator at 100 rpm in darkness at 37 °C in the water bath for 0, 2, 4, 8, 12, 24 h. The reaction was terminated immediately by placing in ice at the end of incubation. The samples were then centrifuged at 10,000 rpm for 40 min, and resulting the supernatant was used for the analysis of the metabolites of phenolic compounds, while the precipitates were used for DNA extraction. The experiments were conducted in triplicate.

UHPLC-Q-TRAP-MS/MS conditions

The identification and quantification of polyphenols from noni fruit and the supernatant from in vitro digestion followed the protocol established by Zhao et al. (2021). UHPLC separation was performed using UPLC-ESI-Q-TRAP-MS (SHIMADZU Nexera X2, Applied Biosystems 4500 QTRAP) equipped with a Waters Acquity UPLC BEH C18 (1.7 μm, 2.1*150 mm). Peak identification was performed in both positive and negative modes. The wavelength was set at 320 nm. The mobile phase A consisted of 0.1 % formic acid in water, and the mobile phase B contained acetonitrile. The column temperature was set to 40 °C, and the auto-sampler temperature was set at 4 °C with an injection volume of 2 μL. The gradient profile was as follows:10 % B (0–0.5 min), 60 % B (0.5–15 min), 98 % B (15–18 min), 10 % B (18–20 min) with a flow rate of 0.3 mL/min. Each sample was injected with a volume of 20 μL. Data acquisition and processing were performed using SCIEX Analyst Work Station Software (Version 1.6.3) and Sciex MultiQuant™3.0.3.

Analysis of 16S rDNA gene sequencing data

Total DNA was extracted using a Tiangen® kit (Tiangen Biochemical Technology, Beijing, China) (Tang et al., 2022). The V3-V4 regions of 16S rDNA gene was amplified using Bakt 341F primers. The procedure of 16S rDNA amplicons preparation followed a standard protocol. The high throughput sequencing was performed on the Illumina MiSeq platform at Biotree Biomedical Technology (Shanghai, China). Paired-ends reads were demultiplexed in QIIME 2 (2023.1). The overlaps were used to splice the double-end data, and quality control and chimeric filtering were performed using DADA2 pipeline (1.16) to obtain high quality clean data. Then, the representative sequences with single-base precision by dereplication were obtained. Then Amplicon Sequence Variants (ASVs) was used to construct class OTU (Operational Taxonomic Units) tables. Taxonomic analysis was performed in QIIME 2 (2022.11.1) using a trained classifier based on SILVA SSU 138 Ref NR 99 sequences and taxonomy. Phylogenetic tree generation, alpha and beta diversity analysis were performed using the align-to-tree-mafffft-fasttree and core-metrics-phylogenetic pipelines of the plugins in QIIME 2 (2022.11).

Data analysis

The simulated digestion-fermentation was performed on samples with biological triplicates. The results were reported as the mean ± standard deviation (SD) of the data from parallel experiments. The statistical significance of the groups was evaluated using analysis of variance (ANOVA), and variations were deemed significant at a p-value

less than 0.05. The statistical analyses were calculated using SPSS software and Origin software (2019), and all figures were calculated in OringinPro 2019C and Excel (2010) software.

Results and discussion

Physical properties of noni fruit at different ripeness levels

As the fruit ripens, hardness of the pulp and seeds, and color of the peel change significantly ($p < 0.05$) (Fig. 1 and Table 1). The fruit gradually softens as the degree of maturity increases, while the hardness of the seeds increased significantly. Noni fruit contains a large amount of pectin, as the fruit ripens, the carboxyl groups of pectin acid can be esterified and form pectin ester, causing the arrangement between plant cells to gradually loosen due to the loss of pectinic acid and calcium pectinate, resulting in the softness (Zhao et al., 2021). In terms of color, both L* and a* decrease and b* increases. L* represents the brightness of the object, indicating that the brightness of the peel kept increasing as the fruit ripens. The a* value gradually increases, indicating that the fruit fades from green to yellow. Similarly, the b* decreases, indicating that the peel changes towards the color of yellow. The change in color is an indicator of fruit ripeness, which could be caused by the degrade of chlorophyll (Ahmed et al., 2021).

Changes of antioxidant activity in noni fruit at different ripeness levels

Different maturity levels have significant impacts on noni polyphenol content and antioxidant activity. TPC, TFC, and antioxidant activity assays (DPPH, ABTS and FRAP) were employed to reflect different aspects of the bioactive compound's potency. As shown in Table 1, TPC and TFC exhibited a gradual increase from unripe to underripe stages, followed by a decrease after ripeness. On the other hand, antioxidant activity increased as the fruit ripened, with the highest DPPH radical scavenging content, ABTS radical scavenging content, and FRAP iron ion chelating capacity observed at the overripe stage. The decline in TPC in overripe fruit could be influenced by reducing compounds other than phenolics, such as alkaloids, vitamin K and terpenes, as identified in UHPLC-Q-TRAP-MS/MS (Table S1). This may be attributed to the fact that Folin-Ciocalteu reagent used in this assay is not specific to only polyphenols but all reducing compounds. Furthermore, TFC measurement specifically focuses on flavonoids, which showed an increase as the fruit ripened. The reduction in TFC at overripe stage could be partially due to the decrease in tannin content after reaching ripeness (Zhong et al., 2022). Conversely, antioxidant activity (DPPH, ABTS, FRAP) reached its peak at overripe stage, indicating that the phenolic compounds accumulated under the actions of antioxidant enzymes during the ripening process, as polyphenols are the primary contributors to antioxidant power. Studies have demonstrated that matured fruit exhibit stronger resistance to oxidative stress compared to unripe fruit (Yue and Han, 2022). These results highlight the changing patterns of the phenolic compounds during noni ripening and provide important information for the development of the noni fruit industry and the further utilization of the fruit resources.

Table 1
Hardness, color index and phytochemical activities of noni fruit at different ripeness levels.

Physical properties	Unripe fruit	Underripe fruit	Ripe fruit	Overripe fruit
Puncture resistance of pulp (N)	2729.3 ± 117.8 ^{a}	2139.0 ± 96.9^{b}	1859.9 ± 68.8^{c}	1484.4 ± 106.5 ^{d}
Puncture resistance of seeds (N)	2890.2 ± 19.6^{c}	5263.9 ± 234.0^{b}	5551.7 ± 58.8^{b}	6059.8 ± 57.3 ^{a}
L*	13.6 ± 2.50 ^{ab}	16.6 ± 0.36^{b}	14.8 ± 2.65^{b}	18.5 ± 0.64 ^{a}
a*	−4.16 ± 0.13^{c}	−1.97 ± 0.80^{b}	−1.61 ± 0.45 ^{ab}	−0.76 ± 0.26 ^{a}
b*	14.6 ± 2.04 ^{a}	11.2 ± 5.95 ^{a}	12.1 ± 4.13 ^{a}	10.1 ± 2.67 ^{a}
TPC	0.45 ± 0.02 ^{d}	0.73 ± 0.03^{c}	1.44 ± 0.11^{a}	0.91 ± 0.04^{b}
TFC	3.21 ± 0.11^{b}	3.61 ± 0.15^{c}	4.24 ± 0.18 ^{a}	2.95 ± 0.22 ^{d}
DPPH	0.67 ± 0.05^{c}	1.01 ± 0.23^{c}	1.53 ± 0.22^{b}	1.93 ± 0.23 ^{a}
ABTS	1.32 ± 0.02^{c}	1.76 ± 0.11^{b}	1.83 ± 0.11^{b}	2.04 ± 0.06 ^{a}
FRAP	24.2 ± 1.16 ^{d}	32.1 ± 0.65^{c}	36.5 ± 1.35^{b}	50.6 ± 1.27 ^{a}

Values are expressed as mean ± standard deviation. Different letters in the same row indicate significant differences ($p < 0.05$). The results of TPC, TFC, DPPH, ABTS and FRAP are expressed as gallic acid equivalent (GAE), mg rutin equivalent (RE), mg Vitamin C equivalent (VCE), mg Vitamin C equivalent (VCE) and g Fe^{2+} per gram of noni on dry weight basis, respectively.

Changes in phenolic components during noni fruit ripening

The major phenolic compounds in noni fruit were identified and quantified by UPLC-ESI-Q-TRAP-MS/MS (Shimazu Nexera X2, Applied Biosystems 4500 QTRAP). Identification and preliminary charscterization of the phenolic compounds was achieved through comparison of retention times and MS/MS spectra with public data or mass spectrometry databases. The chromatogram and the characterization of all tentatively identified polyphenols is presented in Fig. S1 and Table S1 respectively. Table 2 provides a summary of the pertinent data for the major phenols that were quantified, including MS/MS ion fragments, *m/z*, molecular formula, retention times and quantification results. Flavonoid is the major polyphenol exist in noni. The peak at 4.41 min generated characteristic product ions with *m/z* 16.1, 121.1, was identified as brazilin (*m/z* 285.1), which is consistent with the literature (Tong et al., 2013). Brazilin is a bioactive marker that effectively improves glucose metabolism and stimulates glucose transport in cells. It also exhibits significant hypoglycemic effects in streptozotocin-induced diabetic rats. Rutin and salicylic acid were identified at time points of 5.71 and 7.80, which were consistent with the previous study of noni (Wang et al., 2022). Spinosin (*m/z* 608.6) was identified, consistent with previous literature (Sun et al., 2014). Another peak at 6.37 min with a fragment ion at *m/z* 286.9 was tentatively identified as kaempferol rutinoside, with a fragment ion at *m/z* 449, indicating the loss of a glycoside, which is consistent with the result of Chan et al. (2023). These identified phenolic compounds verified the bioactivity of noni polyphenols as dietary supplements.

The phenolic composition varied significantly at different maturity levels. Table 2 reveals that rutin, isorhamnetin-3-*O*-neohesperidin, and kaempferol-3-*O*-rutinoside are the polyphenols with the highest content in noni, while tricetin and brazilin are unique to noni fruit and were reported to be present for the first time. Previous research has suggested that polyphenols in glycosidic form are more stable and exhibit strong free radical-scavenging ability due to their easily-oxidized phenolic hydroxyl groups (Gu et al., 2020). This could explain the high amounts of rutin, isorhamnetin-3-*O*-neohesperidin and kaempferol-3-*O*-rutinoside. Glycosides can better upregulate antioxidant defense responses and promote anti-inflammatory activity (Stobiecki, 2000), indicating the health beneficial impact of noni. With ripening, the antioxidant capacity greatly improved. Some identified flavonoids such as robinetin, isorhamnetin-3-*O*-neohespeidoside and kaempferol-3-*O*-rutinoside decreased slightly with after the ripe stage, which was consistent with the trend of TPC and TFC changes. On the other hand, phenolic acids, such as salicylic acid, accumulated until the overripe stage, confirming the results of antioxidant capacity (DPPH, ABTS and FRAP) and implying a general trend in the changes of phenolic compounds other than the identified ones. Overall, the increase in maturity exacerbates the phenolic alternation and upregulation of antioxidant capacity. Ripe and overripe noni fruits have the highest anoxidant capacity and are therefore suitable for processing and consumption.

Table 2
Characterization and quantification of major identified phenolic compounds in noni fruit at different ripeness levels (μg/kg).

No.	Compound	RT/ min	M	Formula	MS	MS^2	Unripe	Underripe	Ripe	Overripe
1	Brazilin	4.41	286.3	$C_{16}H_{14}O_5$	285.1	16.1, 121.1	0.28 ± 0.02^{b}	0.34 ± 0.02 ^{a}	0.32 ± 0.01^{a}	0.34 ± 0.01^{a}
2	Rutin	5.71	610.5	$C_{27}H_{30}O_{16}$	611.0	84.9, 302.9, 465	3398.4 ± 81.3 ^{a}	3300.2 ± 110.4 ^{a}	2774.5 ± 40.7^{b}	2911.6 ± 76.5^{b}
3	Spinosin	5.69	608.6	$C_{28}H_{32}O_{15}$	607.5	426.9, 606.8	6.46 ± 0.35 ^{a}	5.48 ± 0.13^{b}	3.68 ± 0.23^{c}	3.89 ± 0.08^{c}
4	Robinetin	5.97	302.2	$C_{15}H_{10}O_7$	303.1	136.9, 201.1, 229	1.85 ± 0.07 ^{a}	1.34 ± 0.08^{b}	1.70 ± 0.28 ^{a}	1.15 ± 0.09^{b}
5	Isorhamnetin-3-*O*-neohespeidoside	6.06	624.5	$C_{28}H_{32}O_{16}$	625.5	85.0, 316.9, 478.8	0.36 ± 0.01^{a}	0.21 ± 0.02^{c}	0.24 ± 0.02^{b}	0.12 ± 0.01^{c}
6	Kaempferol-3-*O*-rutinoside	6.37	594.52	$C_{27}H_{30}O_{15}$	595.0	85, 286.9, 449.0	128.62 ± 3.49 ^{a}	132.9 ± 6.40 ^{a}	101.2 ± 1.97^{b}	79.2 ± 5.18^{c}
7	Astragalin	6.52	448.38	$C_{21}H_{20}O_{11}$	449.0	84.9, 152.9, 286.9	23.2 ± 0.92 ^{a}	15.6 ± 1.08^{b}	12.5 ± 0.84^{c}	13.7 ± 0.43^{c}
8	Tricetin	7.52	302.24	$C_{15}H_{10}O_7$	301.1	106.9, 148.9	0.01 ± 0.00^{b}	0.07 ± 0.05 ^{a}	ND	0.02 ± 0.01 ^{ab}
9	Salicylic acid	7.80	138.12	$C_7H_6O_3$	137.0	65.0, 93.0	15.0 ± 0.58^{c}	17.9 ± 0.28^{b}	16.3 ± 1.13 ^{bc}	23.5 ± 2.04^{b}

Values are expressed as mean ± standard deviation. Different letters in the same row indicate significant differences ($p < 0.05$). RT: retention time (min); M: theoretical mass.

Bioaccessible antioxidant activity of noni during in vitro digestion and colonic fermentation

The bioaccessible total polyphenolic content (TPC) (Fig. 2A) and bioaccessible antioxidant capacity (measured by DPPH, ABTS, and FRAP assays, Fig. 2B to D) exhibited a consistent trend. There was a gradual decrease in bioaccessibility from the oral to the small intestinal phase, reaching a peak at approximately 12 h of colonic fermentation, followed by a significant decline.

During the oral digestion phase, the mechanical disruption of the food structure partially releases polyphenols, thereby enhancing their bioaccessibility and increasing their surface area for interaction with digestive enzymes and salivary proteins (Velderrain-Rodríguez et al., 2014). Subsequently, in the gastrointestinal digestion, released polyphenols may undergo partial degradation under the influence of digestive enzymes. During colonic digestion, the bioaccessible antioxidant activities reached their peak at 12 h of fermentation, which could be attributed to the liberation of polyphenols bound to cell wall fibers that were trapped in the food matrix. These polyphenols evade small intestinal digestion by avoiding contact with digestive enzymes, then their release might be facilitated by carbohydrate hydrolases secreted by colonic microorganisms by disrupting the cell wall structure (Dong et al., 2021). The bioaccessible antioxidant ability significantly decreased during the 12–24 h of fermentation, indicating that after complete release, most of the bound polyphenols might have been degraded and decomposed into a series of low molecular weight metabolites (Gu et al., 2020). Similar digestion trends were reported for mung bean polyphenols by Xie et al. (2022) and Dong et al. (2021), where the TPC increased throughout the 0–12 h of colonic digestion process, suggesting the release of polyphenols from the food matrix and the greater bioavailability of these microbial-derived phenolics in the colon.

While the majority of bioaccessible polyphenols in small intestinal are derived from the plant foods, the phenols in the insoluble fraction may be more bioactive after fermentation by microflora. A growing body of evidence suggests that some of these catabolic metabolites can be partially absorbed from the epithelial cells of large intestine and provide further beneficial effects. The phenols combined with dietary fiber can also act as prebiotics with the capability of modulating the composition of the human gut microbiota (Williamson and Clifford, 2017). Thus, the interactions between polyphenols and intestinal flora are significant for the functional activity of noni polyphenols with in the human body.

Changes of bioaccessible phenolic compounds of noni during in vitro digestion and colonic fermentation

The composition of polyphenols released during different stages of digestion is presented in Table 3. Most quantified phenolic compounds showed an increase from the oral phase to the gastric phase. Specifically, rutin, a phenolic compound rich in noni, increased significantly from 5821.2 to 9228.3 μg/kg fruit during the gastric digestion phase, possibly due to its continuous release during the oral phase and enhanced stability of polyphenols under gastric acidic conditions (pH 3) (Acevedo-Fani et al., 2020). In contrast, most polyphenols showed a decline after small intestine treatments, consistent with the trend observed for bioaccessible antixoidant activity, which could be due to polyphenol degradation during small intestinal digestion.

During colonic digestion, most phenolic compounds reached peak levels at 4–12 h of the fermentation, confirming the trends observed for TPC and antioxidant capacity. Phenolic acids such as salicylic acid and pyrogallol reached their highest levels at 8–12 h with 292.5 ± 26.7 μg/kg and 1.94 ± 0.26 μg/kg, respectively. In comparison, flavonoids such as rutin and robinetin declined significantly during colonic fermentation and were not detected within 4 h of the digestion, possibly due to their degradation into metabolites with smaller molecules such as 3-hydroxy-2-methyl-4H-pyran-4-one and 4-hydroxy-3-methoxymandelic acid, which could not be detected before colonic digestion. On the other hand, isorhamnetin-3-*O*-neohesperidin increased during colonic digestion, possibly owing to its relative stable glycosylated polyphenols structure. Isorhamnetin-3-*O*-neohespeidosidel has high medicinal value and antioxidative impact that can promote blood circulation (Gong et al., 2020), suggesting it may be a functional antioxidant in noni worth studying and developing. Overall, the results of phenolic profile of noni fruit during digestion revealed that many polyphenols originating from the fruit were digested during small intestine, while a large amount of fiber-bound polyphenols were released during colonic digestion, metabolized and interact with intestinal microbiota, thereby playing an important functional role in promoting health (Xie et al.,2022).

Alterations in the composition and structure of the intestinal microbiota

Fig. 3 showed the relative abundance and taxonomic profile of colonic microtiota in the noni subjected and blank control groups. Fecal samples were collected at different time points (0 h, 4 h, 8 h, 12 h and 24 h) of the fermentation for DNA sequencing, and alpha and beta diversities were applied to analyze changes in intestinal flora. The majority of the colonic flora comprised Firmicutes, Bacteroidetes, Proteobacteria, and Actinobacteria, accounting for over 90 % of the total intestinal bacteria, which is similar to that of humans (Chen et al.,2021).

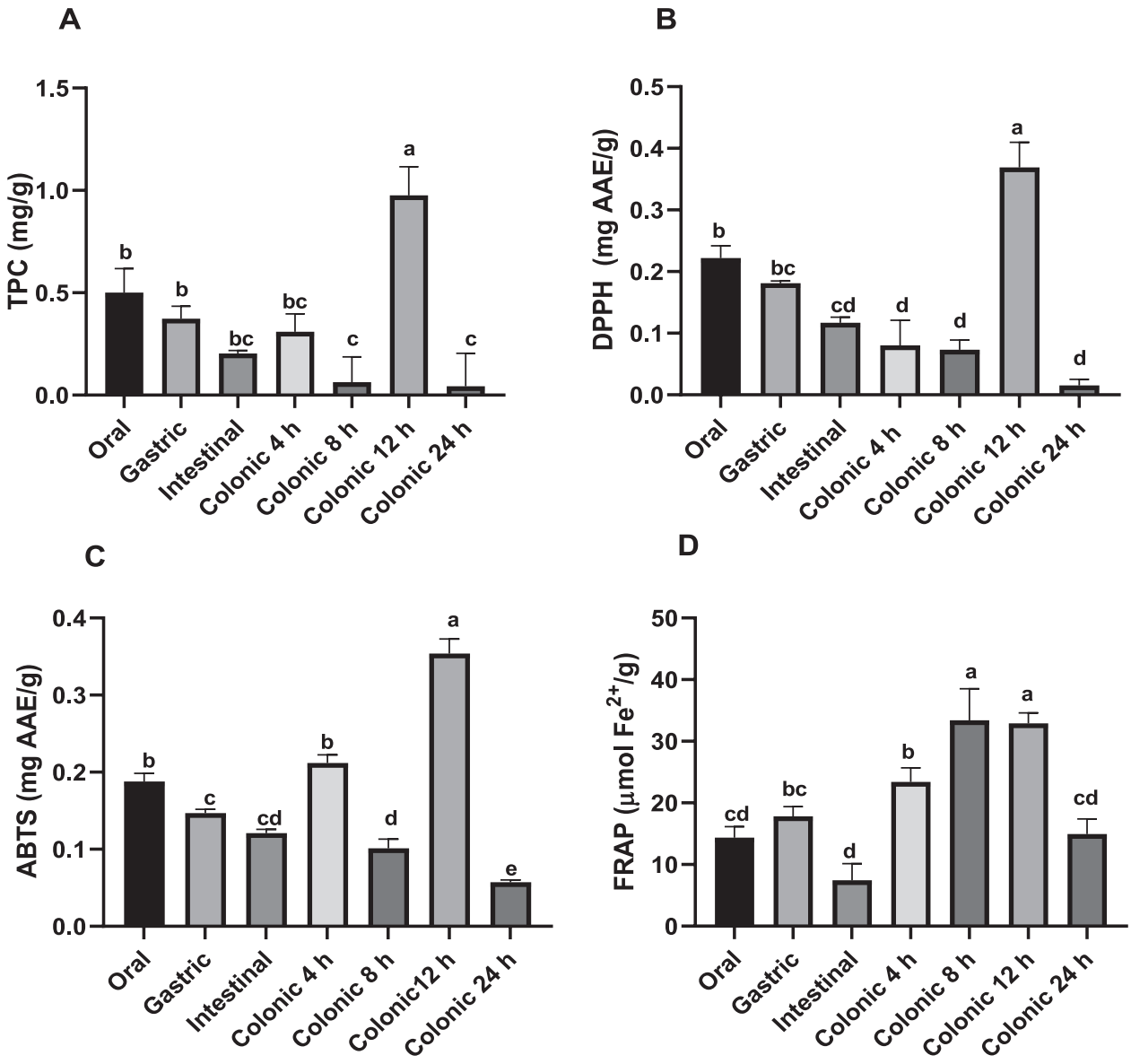

Fig. 2. Bioaccessible total phenolic contents (TPC) and antioxidant capacity of noni fruit subjected to different phases of in vitro digestion and different time points of colonic fermentation (marked by the axis). (A) Total phenolic capacity (TPC); (B) DPPH radical-scavenging activity (DPPH); (C) ABTS scavenging activity (ABTS); (D) Ferric ion reducing antioxidant power (FRAP). The results are expressed as mg gallic acid equivalent (GAE) per gram of noni on dry weight basis, and the results of DPPH and ABTS are expressed as mg ascorbic acid equivalent (AAE) per gram of noni, and the results of FRAP are expressed as μmol Fe^{2+} per gram of noni on dry weight basis. Different letters represent significant difference ($p < 0.05$).

At the phylum level, the experimental group (EX) displayed a decrease in the relative abundance of Firmicutes, while Bacterodetes slowly increased (Fig. 3A). A high ratio of Firmicutes/Bacteroidetes (F/B) is an important indicator of intestinal flora disorders (Stojanov et al., 2020). In the experimental group, a reduced F/B ratio was observed, suggesting that noni may regulate intestinal microbiota with probiotic properties. At the genus level, the relative abundance of intestinal microorganisms in the noni experimental group underwent a significant change (Fig. 3B). Specifically, the relative abundance of *Prevotella* significantly increased. According to previous research, *Prevotella* is associated with pectin metabolism and has the ability to produce short-chain fatty acids (SCFA), paticularly butyrate, which can serve as a source of energy for the host and play an important role in intestinal health (Xu et al., 2020). The results suggest that colonic digestion of noni promote the growth of some beneficial bacteria.

The UniFrac distance-based principal coordinate analysis (PCoA) plot (Fig. 3C) reveals a distinct separation beween the five fermentation groups with noni, particularly the 12 h and 24 h fermentation groups, clustering closely. This indicates noni plays a significant role in modulating the gut microbiota, specifically after 12 h of colonic digestion, which is in line with the results of the variation trend of polyphenols during digestion.

The heatmap (Fig. 3D) shows that the relative abundance of *Escherichia-Shigella*, *Streptococcus* and *Bacteroides* decreased in the experimental groups, while *Blautia*, *Ruminococcus, Lachnospira* increased. Research has demonstrated that *Shigella* spp. is typically associated with low SCFA concentrations and increased metabolic pathways that produce pathogenic and endotoxemia-related substances (Baltazar-díaz, et al., 2022). Conversely, *Ruminococcus* is reported to be a probiotics and related with reduced incidence rates of ulcerative colitis and infantile allergic disease (Nishino, et al., 2018). These findings again underscore the potential functional properties of noni during colonic digestion with increased beneficial bacteria and suppressed pathogens.

The spearman r correlations between the calculated polyphenols and

Table 3
The concentrations of individual polyphenols from noni during in vitro simulated digestion and colonic fermentation (μg/kg).

No.	Compounds	After oral phase	After gastric phase	After Intestinal phase	Colonic fermentation 4 h	8 h	12 h	24 h
1	4-hydroxy-3-methoxymandelic acid	ND	ND	ND	1.46 ± 0.32 ^{d}	2.56 ± 0.44^{c}	3.60 ± 0.13^{b}	5.35 ± 0.12 ^{a}
2	Pyrogallol	ND	ND	0.16 ± 0.07^{b}	1.89 ± 0.20 ^{a}	1.94 ± 0.26 ^{a}	1.73 ± 0.01 ^{a}	1.84 ± 0.02 ^{a}
3	3-hydroxy-2-methyl-4H-pyran-4-one	ND	0.06 ± 0.03^{c}	ND	8.35 ± 1.39 ^{a}	7.88 ± 1.90 ^{ab}	6.37 ± 0.95^{b}	ND
4	Brazilin	0.92 ± 0.14^{b}	2.70 ± 0.57 ^{a}	ND	0.10 ± 0.03^{c}	0.22 ± 0.05^{c}	0.23 ± 0.08^{c}	0.19 ± 0.02^{c}
5	Spinosin	8.69 ± 0.50 ^{a}	11.9 ± 1.65^{b}	ND	2.01 ± 0.32 ^{d}	2.87 ± 0.47 ^{cd}	2.95 ± 0.61 ^{cd}	3.05 ± 0.89 ^{cd}
6	Rutin	5821.2 ± 142.5^{b}	9228.3 ± 96.3 ^{a}	1967.1 ± 105.2^{c}	ND	ND	ND	ND
7	Robinetin	2.70 ± 0.53^{b}	3.35 ± 0.63 ^{ab}	0.73 ± 0.01^{c}	ND	ND	0.09 ± 0.01^{c}	ND
8	Isorhamnetin-3-*O*-neohespeidoside	0.81 ± 0.19^{c}	ND	ND	15.3 ± 1.53 ^{a}	17.2 ± 2.35 ^{a}	14.0 ± 2.30 ^{a}	16.1 ± 3.50 ^{a}
9	Kaempferol-3-*O*-rutinoside	179.1 ± 15.4^{b}	265.3 ± 28.4 ^{a}	45.9 ± 16.2^{c}	ND	ND	ND	ND
10	Astragalin	33.3 ± 4.91^{b}	29.9 ± 3.35^{b}	2.34 ± 0.68^{c}	0.45 ± 0.16^{c}	0.25 ± 0.15^{c}	0.36 ± 0.15^{c}	0.50 ± 0.13^{c}
11	Tricetin	ND	0.05 ± 0.02^{b}	ND	0.04 ± 0.20^{b}	0.26 ± 0.03 ^{a}	0.35 ± 0.03 ^{a}	ND
12	Salicylic acid	129.6 ± 13.3 ^{e}	63.7 ± 2.6^{f}	74.2 ± 2.30^{f}	101.4 ± 2.59^{c}	292.5 ± 26.7 ^{a}	182.7 ± 18.1^{b}	184.7 ± 28.4^{b}

Values are expressed as mean ± standard deviation. Different letters in the same row indicate significant differences ($p < 0.05$). OP: oral phase; GP: gastric phase; IP: intestinal phase; ND: not detected.

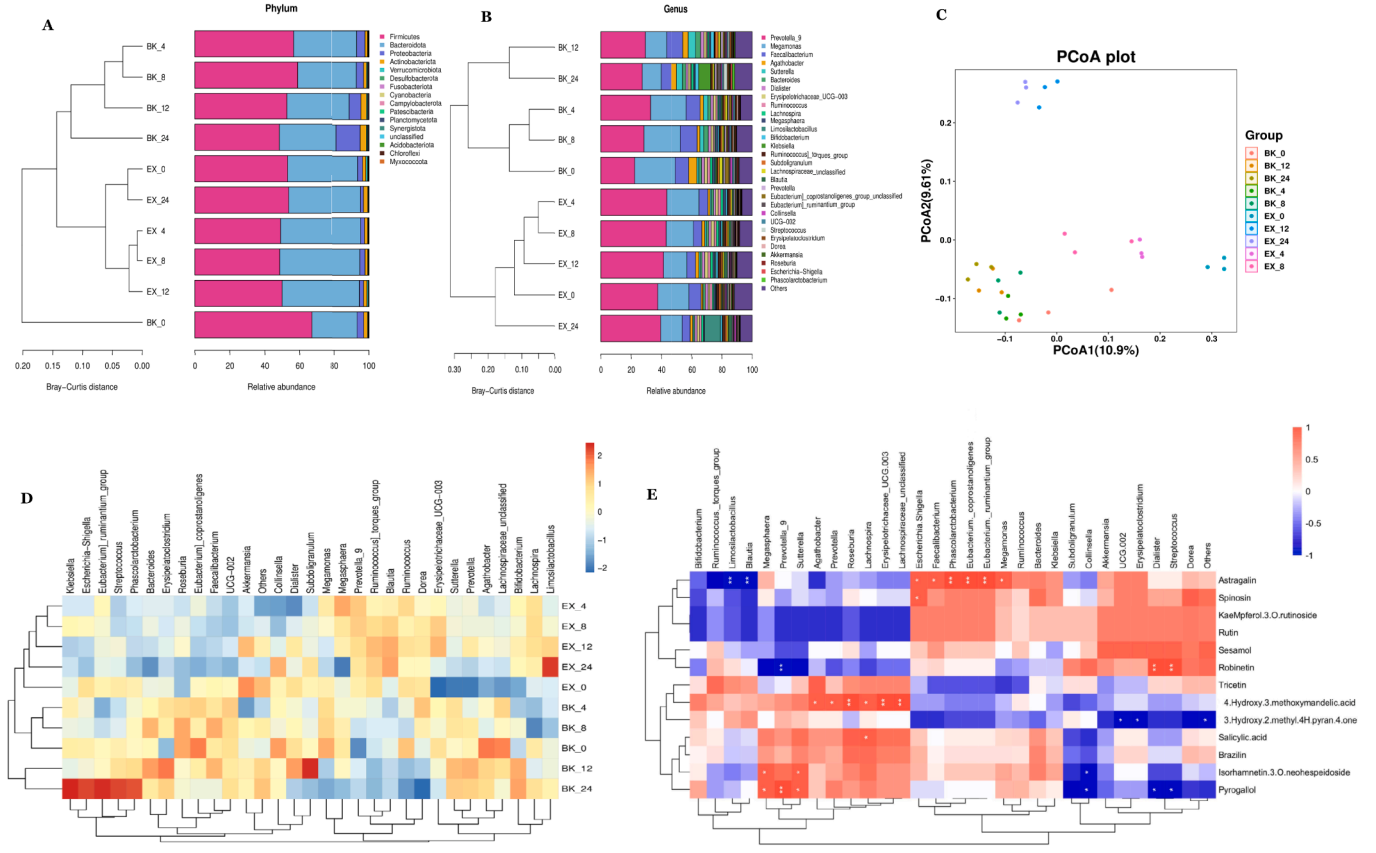

Fig. 3. Microbial diversity and abundance of colonic phase analyzed from control and noni-involved in vitro fecal fermentations at different time points. (A) Bacterial taxonomic profile (Bray-Curtis) at phylum level; (B) Bacterial taxonomic profile (Bray-Curtis) at genus level;(C) PCoA (UniFrac) of all groups. BK: blank control; EX: experimental groups with noni fruit, and the followed numbers indicate time length (hours) of fermentation; (D) Heatmap of microbiota composition at the genus level; (E) Heatmap of the spearman *r* correlations between polyphenols and gut microbiome at the genus level. * and ** Indicates the associations are significant ($p < 0.05$ and $p < 0.01$, respectively).

the major gut microbiome at the genus level were analyzed, and the results are shown in Fig. 3E as a hierarchical clustering heatmap. The findings indicated significant positive or negative correlations between the gut microbiome and the levels of astragalin, 4-hydroxy-3-methoxy-mandelic acid, robinetin, isorhamnetin-3-*O*-neohespeidoside and pyro-gallol. Astragalin, a typical flavonoid in Chinese medicine *Astragalus*, showed highest number of associations with genera compared to other polyphenols, including *Eubacterium coprostanoligenes, Eubacterium ruminantium* group and *Phascolarcotobacterium* ($p < 0.01$ with positive correlations). Specifically, *Eubacterium coprostanoligenes* is known for its cholesterol-reducing ability, while *Phascolarcotobacterium* is associated with intestinal epithelial health due to the production of acetate and

propionate (Yin, et al., 2023). On the other hand, isorhamnetin-3-*O*-neohespeidoside and pyrogallol were found to be negatively related with *Collinsellla* ($p < 0.05$), which is found to be enriched in patients with symptomatic atherosclerosis (Gomez-Arango et al., 2018). Some polyphenols newly produced in the colon, such as 4-hydroxy-3-methoxymandelic acid and pyrogallol, showed significant associations with *Roseburia, Lanchnospiraceae, Erysipelotrichaceae* and *Megasphaera*, suggesting these genera may play a key role in the catabolism of polyphenols during colonic digestion. Among these genera, *Roseburia* is linked with preventing intestinal inflammation and maintaining energy homeostasis by producing metabolites, and *Lanchnospiraceae* is associated with butyric acid production and may offer protection against colon cancer (Vacca et al., 2020). Overall, the alterations observed in the intestinal bacteria indicate that the digestion of noni in the colon may elevate the relative abundance of certain beneficial bacteria while inhibit the growth of specific pathogenic bacteria. These effects on the microbiome may reflect the prebiotic properties of noni polyphenols.

Conclusion

The physical properties and antioxidant activity of noni undergo significant changes during the ripening process, with the peel transitioning from dark green to white, the fruit becoming softer and the seeds becoming harder. Fully-ripened noni fruit displays the strongest antioxidant capacity. During in vitro digestion, polyphenols were gradually released from the oral to the gastrointestinal phase and partially decomposed in the small intestinal compartment due to their structural instability. The release of fiber-bound phenols during the colonic fermentation resulted in a higher bioaccessible antioxidant activity between 8 and 12 h of colonic fermentation, indicating the colon as an important site of utilization for phenols. Intestinal flora promoted the metabolism of phenolics in noni, facilitated the absorption of the polyphenols. Additionally, noni altered the relative abundance and composition of the intestinal flora, reducing the Firmicutes/Bacteroidetes ratio and increasing the relative abundance of *Prevotella* and *Ruminococcus*, which possess prebiotic properties. These findings suggest that noni polyphenols significantly contribute to the health benefits of noni fruit through their absorbable antioxidant capacity and their ability to improve the structure of the intestinal microbiota.

CRediT authorship contribution statement

Juanyun Chen: Formal analysis, Writing – original draft. **Xiaoai Chen:** Data curation, Supervision. **Yanjun Zhang:** Methodology. **Zhen Feng:** Funding acquisition, Methodology. **Kexue Zhu:** Data curation, Funding acquisition. **Fei Xu:** Methodology, Validation. **Chunhe Gu:** Conceptualization, Funding acquisition, Supervision, Writing – review & editing.

Declaration of competing interest

The authors declare that they have no known competing financial interests or personal relationships that could have appeared to influence the work reported in this paper.

Data availability

Data will be made available on request.

Acknowledgements

This work was supported by General Program of Provincial Natural Science Fund of Hainan, China (NO. 322MS136, 322QN399), Central Public-interest Scientific Institution Basal Research Fund (NO. 1630142022006) and Chinese Academy of Tropical Agricultural Sciences for Science and Technology Innovation Team of National Tropical Agricultural Science Center (NO. CATASCXTD202304).

Appendix A. Supplementary data

Supplementary data to this article can be found online at https://doi.org/10.1016/j.fochx.2023.101076.

References

Acevedo-Fani, A., Ochoa-Grimaldo, A., Loveday, S. M., & Singh, H. (2021). Digestive dynamics of yoghurt structure impacting the release and bioaccessibility of the flavonoid rutin. *Food Hydrocolloids, 111*, Article 106215. https://doi.org/10.1016/j.foodhyd.2020.106215

Baltazar-Díaz, T. A., González-Hernández, L. A., Aldana-Ledesma, J. M., Peña-Rodríguez, M., Vega-Magaña, A. N., Zepeda-Morales, A. S. M., & Bueno-Topete, M. R. (2022). Notable intestinal dysbiosis orchestrated by Escherichia/Shigella, decreased levels of SCFTA (short chain fatty acids) and alterations in metabolic pathways characterize patients with alcohol-decompensated cirrhosis in western Mexico. *Annals of Hepatology, 27*, Article 100812. https://doi.org/10.1016/j.aohep.2022.100812

Chan, Y., Huang, J., Wong, H., Li, J., & Zhao, D. (2023). Metabolic fate of black raspberry polyphenols in association with gut microbiota of different origins in vitro. *Food Chemistry, 404*, Article 134644. https://doi.org/10.1016/j.foodchem.2022.134644

Chen, X., Gu, C., Zhu, K., Xu, F., Feng, Z., & Zhang, Y. (2024). Insight into the effects of different ripeness levels on the quality and flavor chemistry of Noni fruit (Morinda citrifolia L.). *Food Chemistry, 434*, Article 137408. https://doi.org/10.1016/j.foodchem.2023.137408

Chen, Y., Zhou, J., & Wang, L. (2021). Role and mechanism of gut microbiota in human disease. *Frontiers in cellular and infection microbiology*, 86. https://doi.org/3389.2023/fmicb.1098386.

Dong, R., Liu, S., Xie, J., Chen, Y., Zheng, Y., Zhang, X., & Yu, Q. (2021). The recovery, catabolism and potential bioactivity of polyphenols from carrot subjected to in vitro simulated digestion and colonic fermentation. *Food Research International, 143*, Article 110263. https://doi.org/10.1016/j.foodres.2021.110263

Fahim, J. R., Attia, E. Z., & Kamel, M. S. (2019). The phenolic profile of pea (Pisum sativum): A phytochemical and pharmacological overview. *Phytochemistry Reviews, 18*(1), 173–198. https://doi.org/10.1007/s11101-018-9586-9

Geng, Z., Wang, J., Zhu, L., Yu, X., Zhang, Q., Li, M., & Yang, X. (2023). Metabolomics provide a novel interpretation of the changes in flavonoids during sea buckthorn (Hippophae rhamnoides L.) drying. *Food Chemistry, 413*, Article 135598. https://doi.org/10.1016/j.foodchem.2023.135598

Gu, C., Suleria, H. A. R., Dunshea, F. R., & Howell, K. (2020). Dietary Lipids Influence Bioaccessibility of Polyphenols from Black Carrots and Affect Microbial Diversity under Simulated Gastrointestinal Digestion. *Antioxidants, 9*(8), 762. https://doi.org/10.1016/j.tifs.2019.09.005

Gomez-Arango, L. F., Barrett, H. L., Wilkinson, S. A., Callaway, L. K., McIntyre, H. D., Morrison, M., & Dekker Nitert, M. (2018). Low dietary fiber intake increases Collinsella abundance in the gut microbiota of overweight and obese pregnant women. *Gut microbes, 9*(3), 189–201. https://doi.org/10.1080/19490976.2017.1406584

Gong, G., Guan, Y. Y., Zhang, Z. L., Rahman, K., Wang, S. J., Zhou, S., … Zhang, H. (2020). Isorhamnetin: A review of pharmacological effects. *Biomedicine & Pharmacotherapy, 128*, Article 110301. https://doi.org/10.1016/j.biopha.2020.110301

Kesavan, P., Banerjee, A., Banerjee, A., Murugesan, R., Marotta, F., & Pathak, S. (2018). An overview of dietary polyphenols and their therapeutic effects. Polyphenols: *Mechanisms of Action in Human Health and Disease*, 221-235. https://doi.org/10.1016/B978-0-12-813006-3.00017-9.

Laya, A., & Koubala, B. B. (2020). Polyphenols in cassava leaves (Manihot esculenta Crantz) and their stability in antioxidant potential after in vitro gastrointestinal digestion. *Heliyon, 6*(3), Article e3567. https://doi.org/10.1016/j.heliyon.2020.e03567

Loo, Y. T., Howell, K., Suleria, H., Zhang, P., Gu, C., & Ng, K. (2022). Sugarcane polyphenol and fiber to affect production of short-chain fatty acids and microbiota composition using in vitro digestion and pig faecal fermentation model. *Food Chemistry, 385*, Article 132665. https://doi.org/10.1016/j.foodchem.2022.132665

Minekus, M., Alminger, M., Alvito, P., Ballance, S., Bohn, T., Bourlieu, C., … Brodkorb, A. (2014). A standardised static in vitro digestion method suitable for food–an international consensus. *Food & function, 5*(6), 1113–1124. https://doi.org/10.1039/c3fo60702j

Motshakeri, M., & Ghazali, H. M. (2015). Nutritional, phytochemical and commercial quality of Noni fruit: A multi-beneficial gift from nature. *Trends in Food Science & Technology, 45*(1), 118–129. https://doi.org/10.1016/j.tifs.2015.06.004

Nishino, K., Nishida, A., Inoue, R., Kawada, Y., Ohno, M., Sakai, S., & Andoh, A. (2018). Analysis of endoscopic brush samples identified mucosa-associated dysbiosis in inflammatory bowel disease. *Journal of gastroenterology, 53*(1), 95–106. https://doi.org/10.1007/s00535-017-1384-4

Pratap, U. P., Hima, L., Priyanka, H. P., & ThyagaRajan, S. (2017). Noni (Morinda citrifolia L.) fruit juice reverses age-related decline in neural-immune interactions in the spleens of old F344 rats. *Journal of ethnopharmacology, 198*, 363–371. https://doi.org/10.1016/j.jep.2017.01.034

Shiu, J. W., Slaughter, D. C., Boyden, L. E., & Barrett, D. M. (2015). Effect of the shear-to-compressive force ratio in puncture tests quantifying watermelon mechanical

properties. *Journal of Food Engineering, 150*, 125–131. https://doi.org/10.1016/j.jfoodeng.2014.11.007

Stobiecki, M. (2000). Application of mass spectrometry for identification and structural studies of flavonoid glycosides. *Phytochemistry, 54*(3), 237–256. https://doi.org/10.1016/j.jpha.2014.01.003

Stojanov, S., Berlec, A., & Štrukelj, B. (2020). The influence of probiotics on the firmicutes/bacteroidetes ratio in the treatment of obesity and inflammatory bowel disease. *Microorganisms, 8*(11), 1715. https://doi.org/10.3390/microorganisms8111715

Sun, S., Liu, H., Xu, S., Yan, Y., & Xie, P. (2014). Quality analysis of commercial samples of ziziphi spinosae semen (suanzaoren) by means of chromatographic fingerprinting assisted by principal component analysis. *Journal of Pharmaceutical Analysis*, 2014, 4 (3): 217-222.

Tailulu, A., Li, M., Ye, B., Al-Qudaimi, R., Cao, F., Liu, W., & Shi, P. (2022). Antimicrobial and anticancer activities of Hainan dry noni fruit alcoholic extracts and their novel compounds identification using UPLC-Q-Exactive Obitrap-MS/MS. *Journal of Pharmaceutical and Biomedical Analysis, 220*, Article 114989. https://doi.org/10.1016/j.jpba.2022.114989

Tang, R., Yu, H., Ruan, Z., Zhang, L., Xue, Y., Yuan, X., & Yao, Y. (2022). Effects of food matrix elements (dietary fibres) on grapefruit peel flavanone profile and on faecal microbiota during in vitro fermentation. *Food Chemistry, 371*, Article 131065. https://doi.org/10.1016/j.foodchem.2021.131065

Tong, X., Zhu, H., Shi, Y., Xu, H., Wang, B., & Zhao, J. (2013). An LC/MS/MS method for simultaneous quantitation of two homoisoflavones: Protosappanin B and brazilin with hypoglycemic activity in rat plasma and its application to a comparative pharmacokinetic study in normal and streptozotocin-treated rats. *Journal of Ethnopharmacology, 148*(2), 682–690. https://doi.org/10.1016/j.jep.2013.05.029

Vacca, M., Celano, G., Calabrese, F. M., Portincasa, P., Gobbetti, M., & De Angelis, M. (2020). The controversial role of human gut lachnospiraceae. *Microorganisms, 8*(4), 573. https://doi.org/10.3390/microorganisms8040573

Velderrain-Rodríguez, G. R., Palafox-Carlos, H., Wall-Medrano, A., Ayala-Zavala, J. F., Chen, C. O., Robles-Sánchez, M., … González-Aguilar, G. A. (2014). Phenolic compounds: Their journey after intake. *Food & function, 5*(2), 189–197. https://doi.org/10.1039/c3fo60361j

Wang, R., Wang, L., Zhang, L., Wan, S., Li, C., & Liu, S. (2022). Solvents effect on phenolics, iridoids, antioxidant activity, antibacterial activity, and pancreatic lipase inhibition activity of noni (Morinda citrifolia L.) fruit extract. *Food Chemistry, 377*, Article 131989. https://doi.org/10.1016/j.foodchem.2021.131989

Williamson, G., & Clifford, M. N. (2017). Role of the small intestine, colon and microbiota in determining the metabolic fate of polyphenols. *Biochemical Pharmacology (2017)*. https://doi.org/10.1016/j.bcp.2017.03.012.

Xie, J., Sun, N., Huang, H., Xie, J., Chen, Y., Hu, X., Dong, R., & Yu, Q. (2022). Catabolism of polyphenols released from mung bean coat and its effects on gut microbiota during in vitro simulated digestion and colonic fermentation. *Food Chemistry, 396*, Article 133719. https://doi.org/10.1016/j.foodchem.2022.133719

Xu, Y., Zhu, Y., Li, X., & Sun, B. (2020). Dynamic balancing of intestinal short-chain fatty acids: The crucial role of bacterial metabolism. *Trends in Food Science & Technology, 100*, 118–130. https://doi.org/10.1016/j.tifs.2020.02.026

Yin, Z., Liu, B., Feng, S., He, Y., Tang, C., Chen, P., … Wang, K. (2023). A Large Genetic Causal Analysis of the Gut Microbiota and Urological Cancers: A Bidirectional Mendelian Randomization Study. *Nutrients, 15*(18), 4086. https://doi.org/10.3390/nu15184086

Yuan, L., Cheng, F., Yi, J., Cai, S., Liao, X., Lao, F., & Zhou, L. (2022). Effect of high-pressure processing and thermal treatments on color and in vitro bioaccessibility of anthocyanin and antioxidants in cloudy pomegranate juice. *Food Chemistry, 373*, Article 131397. https://doi.org/10.1016/j.foodchem.2021.131397

Yue, W., & Han, F. (2022). Effects of monoglucoside and diglucoside anthocyanins from Yan 73 (Vitis vinifera L.) and spine grape (Vitis davidii Foex) skin on intestinal microbiota in vitro. *Food Chemistry, X, 16*, Article 100501. https://doi.org/10.1016/j.fochx.2022.100501

Zhao, L., Zhao, X., Xu, Y., Liu, X., Zhang, J., & He, Z. (2021). Simultaneous determination of 49 amino acids, B vitamins, flavonoids, and phenolic acids in commonly consumed vegetables by ultra-performance liquid chromatography-tandem mass spectrometry. *Food Chemistry, 344*, Article 128712. https://doi.org/10.1016/j.foodchem.2020.128712

Zhong, J., Wang, Y., Li, C., Yu, Q., Xie, J., Dong, R., Xie, Y., Li, B., Tian, J., & Chen, Y. (2022). Natural Variation On Free, Esterified, Glycosylated and Insoluble-Bound Phenolics of Rubus Chingii Hu: Correlation Between Phenolic Constituents and Antioxidant Activities. *Food Research International, 2022*(162), Article 112043. https://doi.org/10.1016/j.foodres.2022.112043